Heliyon 10 (2024) e38068

Contents lists available at ScienceDirect

Heliyon

journal homepage: www.cell.com/heliyon

Research article

Dynamic changes in Beclin-1, LC3B, and p62 in aldose reductase-knockout mice at different time points after ischemic stroke

Jie Li [a,d,1], Zhenqiu Ning [a,c,d,h,1], Xiaoqin Zhong [e,f,1], Dafeng Hu [c], Yu Wang [c], Xiao Cheng [a,b,c,g,**], Minzhen Deng [a,b,c,g,*]

[a] State Key Laboratory of Traditional Chinese Medicine Syndrome/Department of Neurology, The Second Affiliated Hospital of Guangzhou University of Chinese Medicine, Guangdong Provincial Hospital of Chinese Medicine, Guangdong Provincial Academy of Chinese Medical Sciences, Guangzhou, 510006, China

[b] Guangdong Provincial Key Laboratory of Research on Emergency in TCM, Guangzhou, 510120, China

[c] The Second Clinical Medical College of Guangzhou University of Chinese Medicine, Guangzhou, 510120, China

[d] Department of Anesthesiology, The Second Affiliated Hospital of Guangzhou University of Chinese Medicine, Guangzhou, Guangdong Province, 510000, China

[e] The First Clinical Medical College of Guangzhou University of Chinese Medicine, Guangzhou, 510405, China

[f] Department of Rheumatology, Baoan Hospital of Traditional Chinese Medicine Affiliated to Guangzhou University of Chinese Medicine, Shenzhen, 518100, China

[g] State Key Laboratory of Dampness Syndrome of Chinese Medicine/ Department of Neurology, The Second Affiliated Hospital of Guangzhou University of Chinese Medicine, Guangzhou, 510120, China

[h] Department of Anesthesiology, The First Affiliated Hospital of Guangzhou Medical University, China, Guangzhou, 510120, China

ARTICLE INFO

Keywords:
Ischemic stroke
Aldose reductase
Dynamic changes
Autophagy

ABSTRACT

Ischemic stroke is a brain injury caused by cerebral blood circulation disorders and is closely related to oxidative stress. Aldose reductase (AR) is a critical enzyme involved in oxidative stress. Autophagy has previously been found to play a key role in cerebral ischemia–reperfusion injury. However, it is still unclear how autophagy molecules change after cerebral ischemia–reperfusion injury in AR knockout mice ($AR^{-/-}$). A transient middle cerebral artery occlusion (tMCAO) model was generated in $AR^{-/-}$ mice, and the neurological deficit scores of the mice were observed and recorded on Days 1, 3 and 5 after tMCAO. Neuronal damage in the ischemic penumbra was observed by TTC, HE, and Nissl staining. The expression of the autophagy-related molecules Beclin-1, LC3II/I, and P62 as well as that of molecules related to inflammation, oxidative stress, and neurological damage was detected by RT–qPCR, western blotting, and immunofluorescence. Autophagosomes were observed using a transmission electron microscope. Cerebral ischemia–reperfusion injury caused neurological deficits and ischemic infarction in tMCAO mice ($P < 0.01$). Beclin-1, Bcl2/Bax, SOD, GSH-px, P62, PSD95, and TOM20 levels decreased ($P < 0.05$), while IL-6, LC3II/I, and GFAP levels increased ($P < 0.01$) in the $AR^{-/-}$ tMCAO-1d group and the $AR^{-/-}$

* Corresponding author. Department of Neurology, The Second Affiliated Hospital of Guangzhou University of Chinese Medicine, 111 Dade Road, Guangzhou, 510120, China.

** Corresponding author. State Key Laboratory of Traditional Chinese Medicine Syndrome/Department of Neurology, The Second Affiliated Hospital of Guangzhou University of Chinese Medicine, Guangdong Provincial Hospital of Chinese Medicine, Guangdong Provincial Academy of Chinese Medical Sciences, Guangzhou, 510006, China.

E-mail addresses: chengxiaolucky@126.com (X. Cheng), dengmz1@126.com (M. Deng).

[1] Jie Li, Zhenqiu Ning and Xiaoqin Zhong contributed equally to this work.

https://doi.org/10.1016/j.heliyon.2024.e38068
Received 24 May 2023; Received in revised form 31 August 2024; Accepted 17 September 2024
Available online 19 September 2024

tMCAO-3d group, compared to those in the sham group. Beclin-1, Bcl2/Bax, NOX4, GSH-px, P62, and PSD95 levels increased ($P < 0.01$), while IL-6, LC3II/I, and GFAP levels decreased ($P < 0.01$) in the $AR^{-/-}$ tMCAO-5d group compared to those in the $AR^{-/-}$ tMCAO-1d group. Autophagosome formation was observed in tMCAO mice. In summary, the changes in autophagy proteins in the brain tissue of the $AR^{-/-}$ mice after tMCAO were more obvious on Days 1 and 3 after tMCAO. The expression of Beclin-1 and P62 decreased, and the expression of LC3B increased after cerebral ischemia–reperfusion injury in $AR^{-/-}$ mouse brain tissue.

1. Introduction

Stroke, a cerebral dysfunction resulting from an uneven distribution of blood flow to the brain, continues to be the second most common cause of death and disability globally [1]. Ischemic stroke is caused by various biological mechanisms such as oxidative stress, apoptosis, inflammation, blood–brain barrier damage, and autophagy [2]. Currently, the most widely accepted treatment is thrombolytic therapy or thrombolysis to restore blood perfusion to the brain [3] and save the ischemic penumbra or ischemic tissue around the infarct core [4]. Timely treatment of ischemic stroke to maintain brain function is very important.

Autophagy is a cellular process that utilizes lysosomal degradation to remove excess proteins and organelles, preventing cellular dysfunction and damage in various pathological conditions [5]. Recent studies have shown that cells can detect oxidative stress signals in their environment during ischemic and hypoxic conditions, leading to an increase in autophagy [6]. After ischemic stroke, autophagy is activated to clear damaged proteins, and proper autophagy can protect brain function. However, excessive autophagy leads to excessive removal of substances that disrupt normal cell function [7–10]. Our previous study revealed that wild-type (WT) mice that experienced cerebral ischemia–reperfusion injury exhibit an increased degree of autophagy in brain tissues, as evidenced by an increase in the autophagy markers Beclin-1 and LC3B, a decrease in P62, and an increase in autophagic vesicles, as determined by transmission electron microscopy (TEM) [11]. Therefore, although autophagy plays an important role in cell homeostasis, an excessive increase in its activity may have negative consequences.

Aldose reductase (AR) is the first rate-limiting enzyme in the polyol pathway and catalyzes the first step in the conversion of glucose to sorbitol [12]. The accumulation of excessive sorbitol in tissues can cause impaired cellular function [13]. In our previous study, we observed an increase in AR expression in WT mice with transient middle cerebral artery occlusion (tMCAO) [14]. The knockout of AR has been shown to reduce brain tissue edema and improve the infarct size after ischemic stroke [15]. In addition, we found that AR knockout (KO) reduced NADPH oxidase (NOX) expression 3 days after tMCAO in WT mice [14], indicating that AR deletion has a protective effect on alleviating tMCAO-induced neuronal damage. However, this study aimed to investigate changes in the autophagy markers Beclin-1, P62 and LC3B in AR gene knockout ($AR^{-/-}$) mice after cerebral ischemia–reperfusion injury.

In this study, $AR^{-/-}$ mice were used to establish a tMCAO model. We detected changes in damage markers, autophagy markers, and oxidative stress molecules on Days 1, 3, and 5 after tMCAO and described their changes to provide a basis for understanding the molecular mechanisms of autophagy involved in cerebral ischemia–reperfusion injury.

2. Methods and materials

2.1. Experimental animals

A group of twenty 3-month-old male C57BL/6N mice were procured from the Guangdong Medical Animal Experiment Center. (Guangdong, China; certificate no.: SCXK (Yue)2018-0094). $AR^{-/-}$ mice were acquired from Dr. Sookja Kim Chung at the University of Hong Kong and subsequently backcrossed to the 11th generation strain (N11), resulting in congenic mice to the C57BL/6N strain. A total of 60 3-month-old male $AR^{-/-}$ mice of SPF grade were selected for the study. The mice were housed at the Experimental Animal Center of Guangzhou University of Chinese Medicine, and all the experimental procedures were approved by the Animal Ethics Committee at Guangdong Hospital of Traditional Chinese Medicine (No. 2019049).

2.2. tMCAO model

A detailed description of tMCAO model has previously been provided [14]. In this procedure, we exposed the right common carotid, external carotid, and internal carotid arteries and proceeded to ligate the external carotid artery and common carotid artery. After clamping the distal trunk of the internal carotid artery with a vascular clip, we made a small incision in the external carotid artery. After that, through the incision, a nylon monofilament (diameter = 0.26 mm) was gently inserted and advanced into the internal carotid artery, and the proximal end of the internal carotid artery was ligated to secure the line. After a period of 1 h of ischemia, reperfusion of the internal carotid artery was allowed. The sham group underwent the same procedure but without the insertion of the nylon monofilament.

2.3. Neurological scores

The modified Longa score method was used to evaluate the neurological deficits of mice after 24 h of ischemia–reperfusion [11].

The scoring standard for evaluating neurological deficits in mice is as follows: 0 indicates normal walking without any deficits, 1 indicates that the left forepaw is not fully extended, 2 indicates that the mouse leans left when walking flat and can be rotated left, 3 indicates walking in an unstable manner with the whole body shifting to the left, and 4 indicates disturbed consciousness or an inability to walk independently. Based on the neurological scores, the mice were randomly divided into three groups. (n = 15/group): tMCAO-1d group, tMCAO-3d group, and tMCAO-5d group.

2.4. 2,3,5-Triphenyl tetrazolium chloride (TTC) staining

To assess the size of the cerebral infarct area, the mice were euthanized, and their brains were immediately removed and frozen at −20 °C for 10 min. The brains were then sliced into 5 consecutive coronal sections with a thickness of 2 mm and stained with TTC (Cat: T8877, Sigma, USA) at 37 °C for 15 min. The infarct area was photographed using a digital camera and measured using ImageJ software (National Institutes of Health, Bethesda, USA). The slices were then frozen at −80 °C for the next step.

2.5. Hematoxylin and eosin (HE) staining and Nissl staining

The brain tissue was fixed in 4 % paraformaldehyde for 24 h. Next, the tissues were dehydrated, cleared, embedded in paraffin, and cut into 4 mm thick sections. The paraffin sections were then deparaffinized using xylene and alcohol before being stained with HE or Nissl stain solution. The experimental steps were performed strictly in accordance with the manufacturer's instructions for the HE staining process (Cat: DH0006, LEAGENE, China) and the Nissl staining kit (Cat: C0117, Beyotime, China). The slides were left to air dry overnight and then sealed with neutral gum. The morphological structure of the penumbra zone in the cortex of the mice was examined under a 200 × visual field using microscopy (Zeiss, Oberkochen, Germany).

2.6. Estimation of the superoxide dismutase (SOD) and the glutathione peroxidase (GSH-px) levels

Brain tissues were weighed accurately, mixed with ice-cold PBS at a ratio of 1:9 and homogenized in an ice bath. The samples were then centrifuged at 10,000×*g* for 15 min at 4 °C to obtain the supernatant. SOD and GSH-px levels were assayed according to the manufacturer's instructions for the SOD assay kit (Cat: A001-3-2, Nanjing Jiancheng Biotechnology Co., Ltd, China) and GSH-px assay kit (Cat: A005-1-2, Nanjing Jiancheng Biotechnology Co., Ltd, China), respectively. The results are expressed as units per milligram of total protein (U/mg).

2.7. Reverse transcription quantitative real-time PCR (RT−qPCR) analysis

A tissue RNA purification kit (for adipose tissue) (EZB-RN001A) was purchased from Suzhou Yuingze Biological Medicine Technology Co., Ltd. An Evo M-MLV RT Mix kit with gDNA Clean Buffer for qPCR Ver.2 (Cat: AG11728) and a SYBR Green Premix Pro Taq HS qPCR Kit (Cat: AG11701) were purchased from Accurate Biotechnology (Hunan) Co., Ltd. The gene primers for Beclin-1, interleukin-6 (IL-6), B-cell lymphoma −2 (Bcl-2), Bcl-2-associated X protein (Bax), NOX4, and β-actin were designed and synthesized by Shengong Bioengineering (Shanghai) Co., Ltd. RNA was extracted according to the manufacturer's instructions and its concentration was measured. gDNA removal was performed at 42 °C for 2 min, followed by reverse transcription at 37 °C for 15 min and 85 °C for 5 s qPCR was carried out for 40 cycles with the following conditions: 95 °C for 30 s, extension at 95 °C for 5 s, and 60 °C for 30 s. The relative mRNA levels were calculated using the $2^{-\Delta\Delta CT}$ method. The primer sequences are listed in Table 1.

2.8. Western blot analysis

The tissues were accurately weighed, RIPA lysis buffer (Cat: P0013B, Beyotime, China) containing protease inhibitor (Cat: 5892791001, Merck, Germany) was added, and the samples were then centrifuged at 12000 g at 4 °C for 10 min. The protein

Table 1
Primer sequences.

Gene		Primer sequences (5′-3′)	Length(bp)
Beclin-1	F	GCTGTAGCCAGCCTCTGAAA	80
	R	AATGGCTCCTGTGAGTTCCTG	
IL-6	F	GACAAAGCCAGAGTCCTTCAGA	76
	R	TGTGACTCCAGCTTATCTCTTGG	
Bcl2	F	GCGTCAACAGGGAGATGTCA	138
	R	GCATGCTGGGGCCATATAGT	
Bax	F	GAACCATCATGGGCTGGACA	101
	R	GGTCCCGAAGTAGGAGAGGA	
NOX4	F	AGTGTTTAAGCATTTTCAAACTCCC	144
	R	GAAAGTTGCCAAACAACAGGC	
β-actin	F	ACACTCTCCCAGAAGGAGGG	147
	R	TTTATAGGACGCCACAGCGG	

concentration was measured with a NanoDrop 2000 spectrophotometer (Thermo Fisher, USA). SDS–PAGE loading buffer (Cat: CW0027S, Beijing ComWin Biotech Co., Ltd., China) was added to the sample, and the mixture was boiled for 10 min. The total proteins were separated using 12.5 % SDS–PAGE (Cat: PG113, Shanghai Epizyme Biomedical Technology Co., Ltd., China) and transferred to PVDF membranes (0.2 μm, Millipore, Germany) for 65 min. Blocking in BSA was carried out for 2 h, and the membranes were incubated with the following primary antibodies: Beclin-1 (1:1000, ab207612, Abcam, USA), LC3B (1:1000, ab192890, Abcam, USA), P62 (1:20000, ab109012, Abcam, USA), PSD95 (1:10000, 20665-1-AP, Proteintech, USA), GFAP (1:10000, ab7260, Abcam, USA), and GAPDH (1:5000, ab8245, Abcam, USA), overnight at 4 °C. Following overnight incubation, the membranes were washed with Tris-buffered saline with Tween (TBST) and incubated with an HRP-conjugated secondary antibody (1:5000, ab288151, Abcam, USA or 1:5000, ab205719, Abcam, USA) for 1 h at room temperature. Finally, the membranes were developed with an enhanced chemiluminescence (ECL) reagent kit (Cat: Wbuls0500, Millipore, Germany) and analyzed with imaging equipment (ChemiDoc XRS, Bio-Rad, PA, USA).

2.9. Immunofluorescence analysis

Following paraffin embedding of the tissues, serial 4 mm coronal sections were cut with a microtome. The sections were deparaffinized in xylene and then washed with a graduated series of alcohols. A solution containing 3 % hydrogen peroxide (H_2O_2) was used to quench the endogenous peroxidase activity for 10 min. Next, the sections were heated with sodium citrate thermal antigen repair solution at 90 °C for 10 min, cooled in water and immersed in phosphate-buffered saline (PBS) for 5 min. Beclin-1 (1:100, ab62557, Abcam, USA), LC3B (1:50, ab192890, Abcam, USA), P62 (1:100, ab56416, Abcam, USA) and TOM20 (1:100, 11802-1-AP, Proteintech, USA) antibodies were added and incubated overnight at 4 °C. The next day, the sections were incubated with secondary antibodies (1:200, ab150078, Abcam, USA) (1:200, ab150077, Abcam, USA; or 1:200, ab150113, Abcam, USA) at room temperature for 1 h in a dark room. The cells were incubated with DAPI (P00131, Beyotime, China) at 37 °C for 5 min and rinsed with PBS 3 times. The fluorescence intensity and location of the four proteins were quantified using a fluorescence-inverted microscope (Zeiss, Oberkochen, Germany). Later, quantitative analysis was performed using ImageJ software (National Institutes of Health, Bethesda, USA).

2.10. TEM

The ischemic penumbra of fresh brain tissue was fixed in a 1 mm^3 volume to 2.5 % glutaraldehyde electron microscope (Cat: 2190114, Ted Pella, Inc., USA) fixative at 4 °C. The brain tissues were rinsed three times with PBS. The cells were then fixed in a 1 % osmium solution at 4 °C for 1 h. Next, the cells were dehydrated in a gradient ethanol series, and the ethanol was replaced with acetone. The tissue blocks were permeabilized and finally embedded in epoxy resin. Following polymerization at 80 °C for 24 h, the tissue blocks were transformed into ultrathin sections with a thickness of 60–100 nm. These sections were then double-stained with 3 % lead citrate-dioxide acetate and observed via TEM to detect the presence of autophagic vesicles in the ischemic penumbra.

2.11. Statistical analysis

Statistical calculations were performed with GraphPad Prism 6.0 software. The data are expressed as the mean ± SEM. One-way ANOVA followed by Tukey's post hoc test was used for comparisons among multiple groups. Correlations among Beclin-1, NOX4, GSH-px, P62, and TOM20 expression were analyzed by Pearson correlation, while correlations among Bcl-2/Bax, IL-6, SOD, PSD95, GFAP, and LC3B expression were analyzed by Spearman correlation; $P < 0.05$ indicated significant differences.

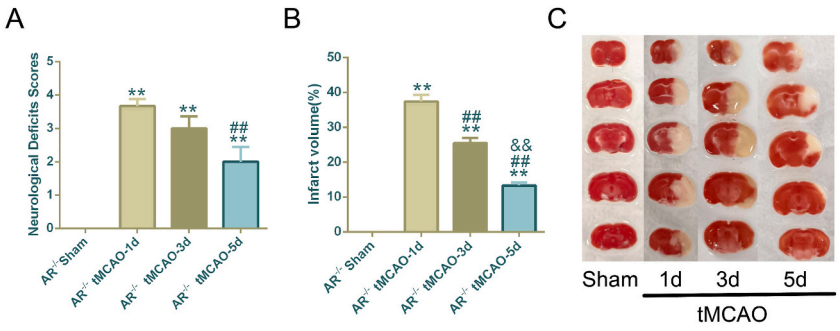

Fig. 1. Neurological functional deficits and cerebral infarction in $AR^{-/-}$ mice after tMCAO. The findings of our study indicate that $AR^{-/-}$ mice experience significant neurological impairment as a result of brain ischemia-reperfusion injury. The tMCAO-1d group exhibited the most severe area of cerebral infarction. However, with increased survival time after tMCAO, the symptoms of nerve damage decreased. A: Neurological deficit scores of $AR^{-/-}$ mice after tMCAO. N = 6; B: Cerebral infarction area after tMCAO in the different groups of $AR^{-/-}$ mice, N = 6; C: Representative TTC-stained sections. The white area represents the cerebral infarction while the red area represents the healthy brain tissue. $^{**}P < 0.01$ vs. the $AR^{-/-}$ sham group, $\#\#P < 0.01$ vs. the $AR^{-/-}$ tMCAO-1d group, and $\&\&P < 0.01$ vs. the $AR^{-/-}$ tMCAO-3d group. (For interpretation of the references to color in this figure legend, the reader is referred to the Web version of this article.)

3. Results

3.1. Neurological functional deficits and cerebral infarction in $AR^{-/-}$ mice after ischemic stroke

Neural function scores were computed for each group of mice using the Longa score method. The findings indicated that the tMCAO mice demonstrated more severe neurological impairment compared to the sham group ($P < 0.01$) (Fig. 1A). This was particularly noticeable at 1 d and 3 d postischemic stroke, with symptoms such as hemiplegia, falling to the paralyzed side while walking, and loss of consciousness observed in the tMCAO mice. The tMCAO procedure successfully induced symptoms of unilateral paralysis similar to those observed in ischemic stroke patients. The brain infarction volume in the tMCAO group was markedly increased ($P < 0.01$) (Fig. 1B and C). Compared with that in the tMCAO-1d group, the infarct volume was decreased in the tMCAO-3d group and tMCAO-5d group ($P < 0.01$). Compared with that in the tMCAO-3d group, the infarct volume was decreased in the tMCAO-5d group ($P < 0.01$). These results indicate that tMCAO causes neurological damage in $AR^{-/-}$ mice, which is most severe on the first postoperative day.

3.2. Histochemical changes in the ischemic penumbra after ischemic stroke in $AR^{-/-}$mice

Previous research has demonstrated that cerebral ischemia can lead to significant naturopathic damage and morphological changes. To investigate the impact of AR knockout on neuropathic damage, HE and Nissl staining were utilized. The sham group exhibited no neuronal necrosis and normal histopathology on HE staining. In contrast, the tMCAO group displayed disordered cell arrangement and neuronal necrosis. (Fig. 2A). Similarly, significant morphological changes, such as nuclear shrinkage, neuronal loss, and dark staining, were detected in the ischemic penumbras of the tMCAO group (Fig. 2B). Histochemical analysis revealed that the most severe neuronal damage in the $AR^{-/-}$ mice caused by tMCAO occurred on the first day after surgery.

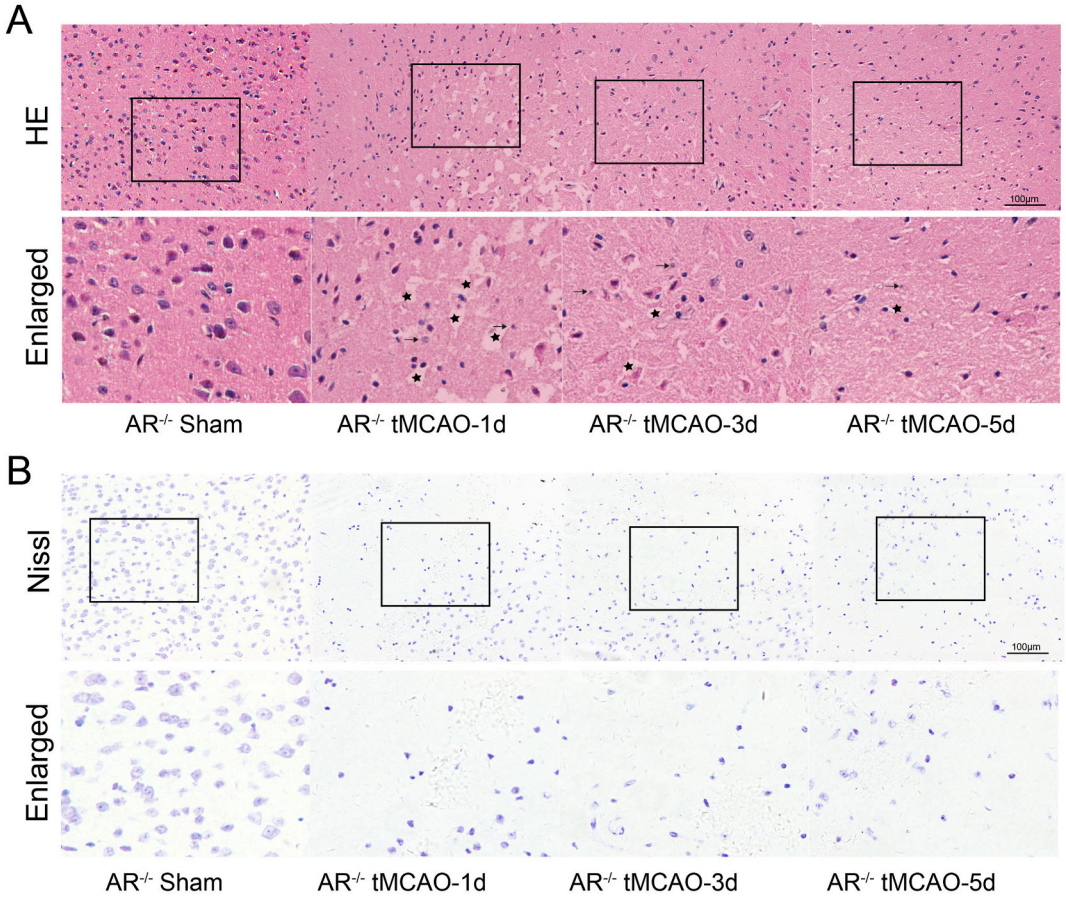

Fig. 2. Histology was evaluated by HE and Nissl staining of the ischemic penumbra at different time points. In this study, we utilized HE and Nissl staining to identify neuronal cell loss and investigate the impact of AR KO on tMCAO-induced neuronal injury in mice. A: Photomicrographs of HE staining of the ischemic penumbra. In the tMCAO model groups, the brain tissue appeared to be loosely structured with water accumulation (★). Additionally, the nuclei of neurons were observed to be shrunk (↑) and trachychromatic (n = 3). B: Nissl staining showed a decrease in the number of neurons in the tMCAO group (n = 3). Scale bar = 100 μm.

3.3. The mRNA expression of Beclin-1, IL-6, Bcl-2/Bax and NOX4 in $AR^{-/-}$ mice was determined by RT–qPCR

The mRNA expression of Beclin-1 and Bcl-2/Bax were significantly lower in the tMCAO-1d and tMCAO-3d groups than in the sham group ($P < 0.01$). Beclin-1 and Bcl-2/Bax expression was significantly greater in the tMCAO-5d group than in the tMCAO-1d group ($P < 0.01$). In contrast, the IL-6 concentration was significantly greater in the tMCAO-1d group and the tMCAO-3d group compared to the sham group ($P < 0.01$); the IL-6 concentration was significantly lower in the tMCAO-5d group than in the tMCAO-3d group ($P < 0.01$). NOX4 expression was significantly greater in the tMCAO-3d group and the tMCAO-5d group compared to the sham group and the tMCAO-1d group ($P < 0.01$) (Fig. 3).

3.4. The levels of SOD and GSH-px in $AR^{-/-}$ mice after ischemic stroke

SOD and GSH-px levels were significantly lower in the ischemic penumbra of the tMCAO-1d group and tMCAO-3d group compared with the sham group ($P < 0.05$). In addition, the level of GSH-px was greater in the tMCAO-5d group compared to the tMCAO-1d group ($P < 0.01$) (Fig. 4). The antioxidant levels in the $AR^{-/-}$ mice were the lowest on the first postoperative day and then gradually recovered on the fifth postoperative day.

3.5. The expression of Beclin-1, LC3II/I, P62, PSD95, and GFAP in mice after ischemic stroke was determined by Western blot analysis

Compared to those in the sham group, the protein levels of Beclin-1 in the ischemic penumbra of the tMACO-1d group of WT mice were significantly greater ($P < 0.05$), while the protein levels of PSD95 were significantly lower ($P < 0.05$) (Fig. 5A and B). Furthermore, we detected $AR^{-/-}$ mouse protein expression after tMCAO using western blotting. Compared with those in the sham group, the expression levels of Beclin-1, P62, and PSD95 in the tMCAO-1d and tMCAO-3d groups were significantly lower ($P < 0.01$), while the expression of LC3II/I in the tMCAO-1d group and the expression of GFAP in the tMCAO-1d and tMCAO-3d groups were significantly greater ($P < 0.01$) (Fig. 5C–F). Compared with those in the tMCAO-1d group and the tMCAO-3d group, the P62 and PSD95 expression levels in the tMCAO-5d group were significantly greater ($P < 0.05$) (Fig. 5F and G). Compared with those in the tMCAO-1d group, the levels of LC3II/I and GFAP expression in the tMCAO-5d group were significantly lower ($P < 0.01$) (Fig. 5E and H). The

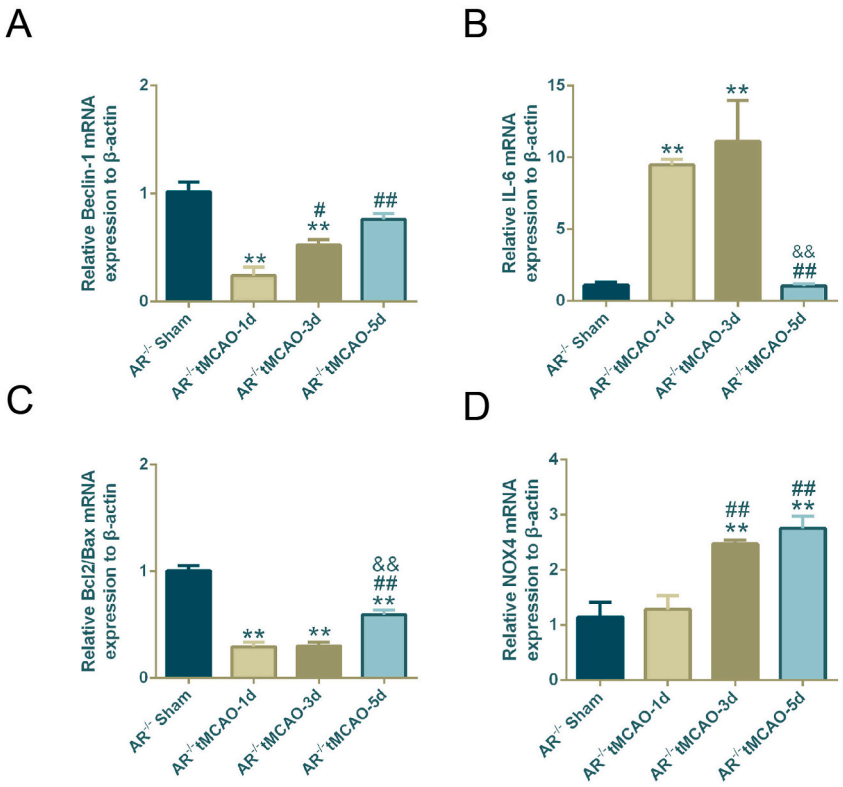

Fig. 3. The mRNA expression of Beclin-1, IL-6, Bcl-2/Bax, and NOX4 in the ischemic penumbra of $AR^{-/-}$ mice after tMCAO. After ischemic stroke, the mRNA expression of Beclin-1 (A) and Bcl-2/Bax (C) was decreased in the ischemic penumbra of $AR^{-/-}$ mice, while the expression of IL-6 (B) and NOX4 (D) was increased. However, the mRNA expression of IL-6 was elevated in the tMCAO-1d and tMCAO-3d groups and decreased in the tMCAO-5d group compared with the $AR^{-/-}$ sham group ($P < 0.01$). N = 6. $^{**}P < 0.01$ vs. the $AR^{-/-}$ sham group, $\#P < 0.05$ vs. the $AR^{-/-}$ tMCAO-1d group, $\#\#P < 0.01$ vs. the $AR^{-/-}$ tMCAO-1d group, and $\&\&P < 0.01$ vs. the $AR^{-/-}$ tMCAO-3d group.

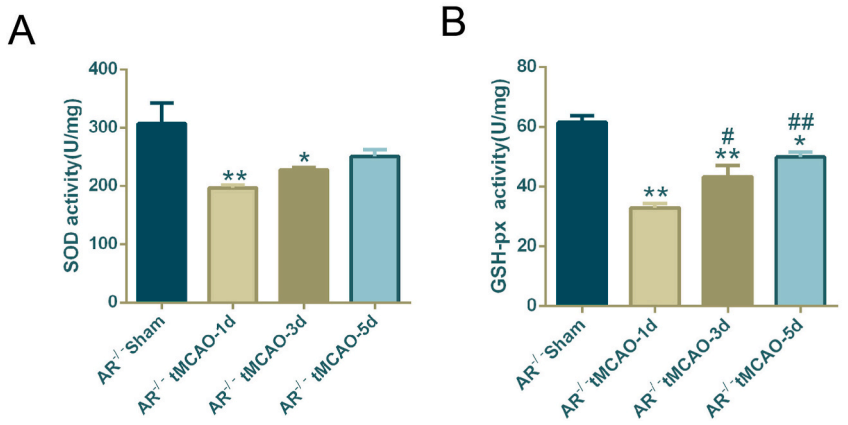

Fig. 4. SOD and GSH-px levels in the ischemic penumbra of $AR^{-/-}$ mice after tMCAO. The levels of SOD (A) and GSH-px (B) were decreased in the ischemic penumbra of the $AR^{-/-}$ mice after tMCAO. In particular, the protein concentrations of SOD and GSH-px were decreased in both the tMCAO-1d and tMCAO-3d groups compared to those in the sham group ($P < 0.05$). N = 6. *$P < 0.05$ vs. the $AR^{-/-}$ sham group, **$P < 0.01$ vs. the $AR^{-/-}$ sham group, #$P < 0.05$ vs. the $AR^{-/-}$ tMCAO-1d group, and ##$P < 0.01$ vs. the $AR^{-/-}$ tMCAO-1d group.

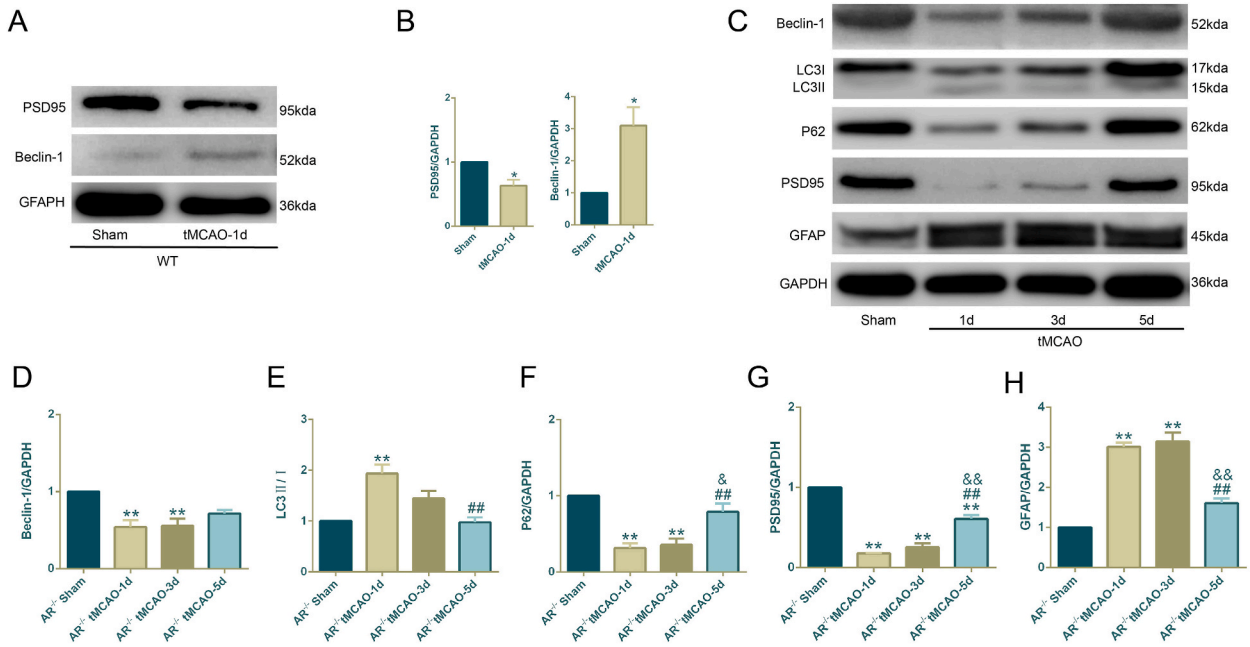

Fig. 5. Western blotting was used to determine Beclin-1, LC3II/I, P62, PSD95, and GFAP expression in the ischemic penumbra. Western blot analysis of Beclin1 and PSD95 in wild-type mice (A, B). The expression of Beclin-1 (D), LC3II/I (E), P62 (F), PSD95 (G), and GFAP (H) in the $AR^{-/-}$ mice was measured by western blotting. N = 3, *$P < 0.05$ vs. the $AR^{-/-}$ sham group, **$P < 0.01$ vs. the $AR^{-/-}$ sham group, ##$P < 0.01$ vs. the $AR^{-/-}$ tMCAO-1d group, &$P < 0.5$ vs. the $AR^{-/-}$ tMCAO-3d group, and &&$P < 0.01$ vs. the $AR^{-/-}$ tMCAO-3d group.

expression of Beclin-1, P62 and PSD95 were decreased in the $AR^{-/-}$ mice after tMCAO, indicating that cerebral ischemia affects the initiation of autophagy and damages the postsynaptic membrane. In addition, protein changes were significant within 3 days after tMCAO and gradually improved on the fifth day.

3.6. The expression of Beclin-1, LC3B, p62 and TOM20 in the $AR^{-/-}$ mice was determined by immunofluorescence analysis

Compared to those in the sham group, the expression levels of Beclin-1, P62, and TOM20 were notably decreased in the tMCAO-1d group and tMCAO-3d group ($P < 0.05$) (Fig. 6A, C,6D). LC3B fluorescence was significantly greater in the tMCAO-1d group and the tMCAO-3d group than in the sham group ($P < 0.01$); LC3B expression was significantly lower in the tMCAO-5d group than in the tMCAO-1d group and the tMCAO-3d group ($P < 0.01$) (Fig. 6B).

3.7. TEM results

No autophagic vesicles were found in the brain tissue of the sham group. The morphology of autophagic vesicles can be seen in the cerebral ischemic penumbra of mice in the tMCAO group. In the tMCAO-1d group, the inner membrane of the neurons was more heavily wrinkled, and autophagic vesicles were more common. There were fewer autophagic vesicles in the neurons of the tMCAO-3d group and tMCAO-5d group (Fig. 7).

3.8. Correlation analysis results

Beclin-1 levels were positively correlated with Bcl-2/Bax, SOD, GSH-px, PSD95, and TOM20 levels (0.792, 0.664, 0.771, 0.817, and 0.756, respectively) ($P < 0.01$). Conversely, Beclin-1 levels were negatively correlated with IL-6, GFAP, and LC3B levels (−0.721, −0.761, and −0.727, respectively) ($P < 0.01$) (Table 2).

4. Discussion

This study established an $AR^{-/-}$ mouse tMCAO model to explore the changes in autophagy markers in brain tissue on Days 1, 3, and 5 after cerebral ischemia and reperfusion in mice, supplemented by the detection of inflammation, oxidative stress, and synaptic damage-related molecules. $AR^{-/-}$ mice exhibited the most severe neuronal damage 1 day after tMCAO, with increased levels of inflammation, oxidative stress and synaptic damage markers. The expression of the autophagy markers Beclin-1 and P62 in brain tissue was reduced, and the expression of LC3B was increased on the first day after tMCAO. On the fifth day after tMCAO, the brain damage in

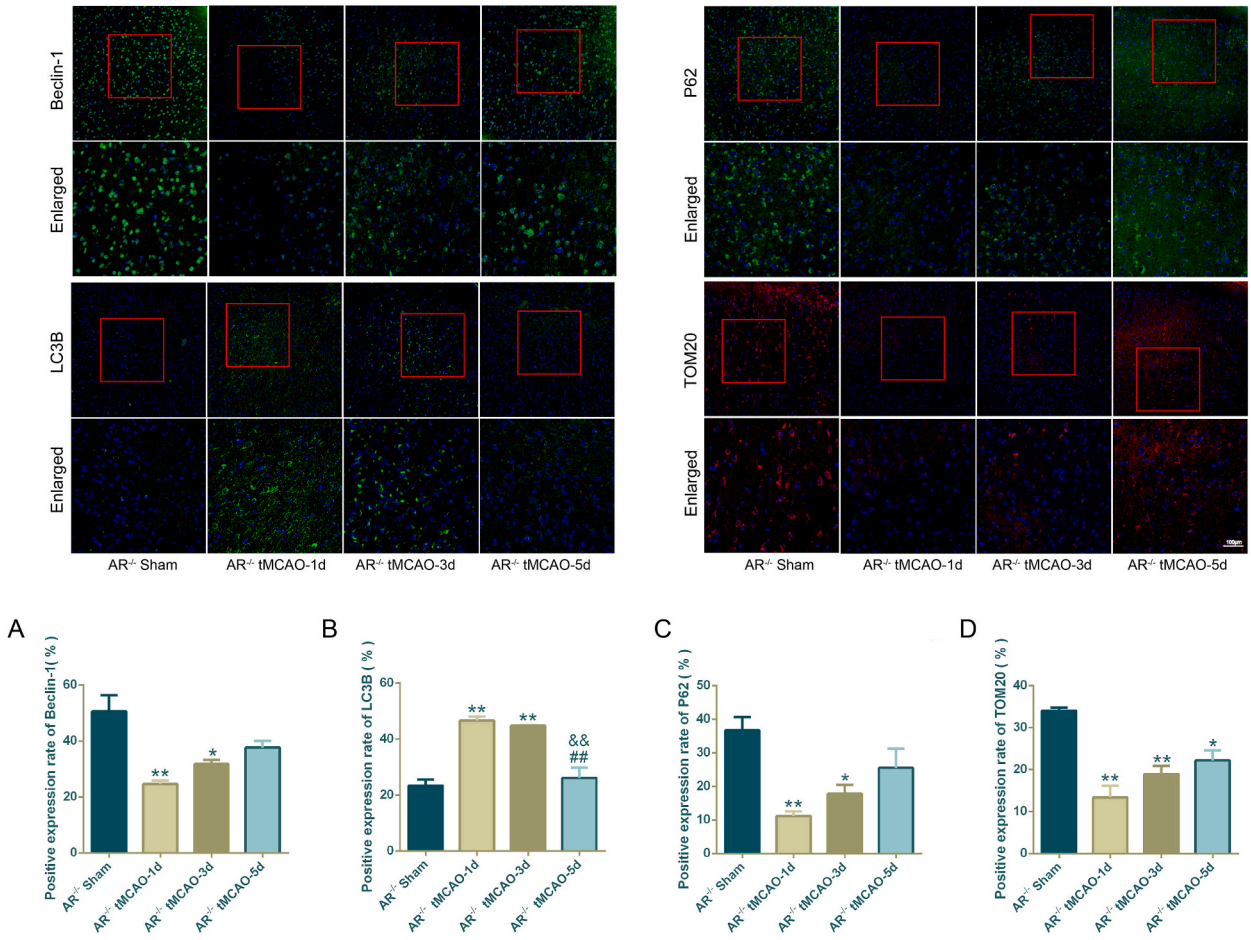

Fig. 6. Immunofluorescence analysis of Beclin-1, LC3B, P62, and TOM20. The expression of Beclin-1 (A), P62 (C), and TOM20 (D) was reduced, but the expression of LC3B (B) was increased in the ischemic penumbra of the $AR^{-/-}$ mice after tMCAO. The blue color in the image represents cell nuclei that were stained with DAPI, while the green or red color indicates a positive expression. The scale bar is 100 μm. N = 3. *$P < 0.05$ vs. the $AR^{-/-}$ sham group, **$P < 0.01$ vs. the $AR^{-/-}$ sham group, ##$P < 0.01$ vs. the $AR^{-/-}$ tMCAO-1d group, and &&$P < 0.01$ vs. the $AR^{-/-}$ tMCAO-3d group. (For interpretation of the references to color in this figure legend, the reader is referred to the Web version of this article.)

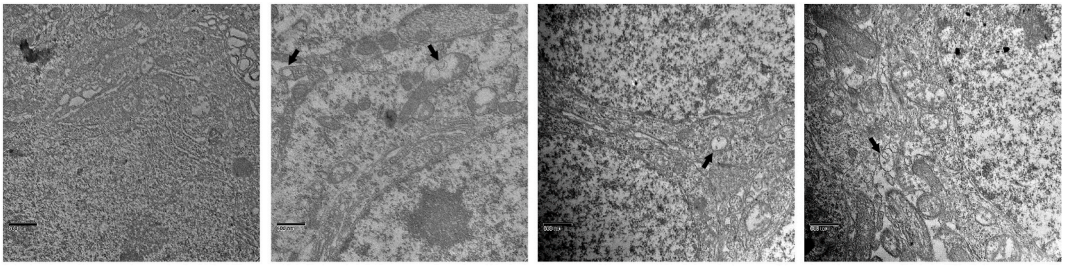

Fig. 7. The number of autophagosomes at different time points after tMCAO determined by TEM in the $AR^{-/-}$ mice. TEM was used to observe autophagosomes in the ischemic penumbra of $AR^{-/-}$ mice following tMCAO. In comparison, the organelles of the sham group appeared normal under TEM, and no significant changes in autophagy were detected. However, in the tMCAO groups, few autophagic vesicles were detected in the neuronal cells. The magnification of this image is 30,000 times (scale bar = 600 nm).

Table 2
Correlation analysis.

	Beclin-1	Bcl2/Bax	IL-6	NOX4	SOD	GSH-px	PSD95	GFAP	LC3B	P62	TOM20
Beclin-1	1	0.792**	-0.721**	-0.103	0.664**	0.771**	0.817**	-0.761**	-0.727**	0.096	0.756**
Bcl2/Bax		1	-0.785**	-0.316	0.622**	0.733**	0.937**	-0.810**	-0.832**	0.671*	0.678*
IL-6			1	0.127	-0.622**	-0.595**	-0.873**	0.761**	0.755**	-0.727**	-0.678*
NOX4				1	-0.123	-0.195	-0.211	0.514	0.343	0.034	-0.307
SOD					1	0.711**	0.852**	-0.831**	-0.888**	0.832**	0.888**
GSH-px						1	0.746**	-0.768**	-0.748*	0.874**	0.918**
PSD95							1	-0.844**	-0.817**	0.732**	0.725**
GFAP								1	0.789**	-0.718**	-0.761**
LC3B									1	-0.622*	-0.727**
P62										1	0.854**
TOM20											1

Note: *P<0.05, **P<0.01

the $AR^{-/-}$ mice was partially relieved.

This study revealed significant changes in the expression of inflammatory and apoptotic indicators, namely, IL-6, GFAP, and Bcl-2/Bax, at 1 and 3 days after tMCAO. During the acute phase, monitoring IL-6 levels is crucial for assessing brain function and neurological status [16]. There is a direct correlation between elevated levels of IL-6 and the severity of stroke, as well as the likelihood of early neurological deterioration, larger infarct size, and poorer clinical outcomes [17,18]. Reducing IL-6 levels after stroke may be an effective treatment for ischemic stroke to mitigate inflammatory responses. GFAP is a marker of astrocytes that can regulate synaptic transmission and protect against synaptic dysfunction after stroke-related brain injury [19]. Astrocytes play a crucial role in the ischemic penumbra by releasing neurotrophic factors that aid in the restoration and reconstruction of damaged neurons and blood vessels [20]. GFAP is a key player in the pathogenesis of ischemic stroke. The apoptotic process, reflected by Bcl-2/Bax expression, is a major cause of neuronal death following cerebral ischemia–reperfusion. Bcl-2 attenuates apoptosis, while Bax promotes it [21]. Reducing neuronal apoptosis has been found to be effective in reducing brain damage. After ischemic stroke, patients exhibit reduced levels of antiapoptotic proteins, which can lead to neuronal apoptosis and increase the risk of physical deterioration [22]. Our study revealed that the levels of the inflammation-related indicators IL-6 and GFAP were significantly greater on Day 3 after tMCAO than in the $AR^{-/-}$ sham group. Additionally, the apoptosis-related indicator Bcl-2/Bax was significantly decreased in the tMCAO group. Interestingly, compared to those in a previous study [11], IL-6 and GFAP expression decreased rapidly in the $AR^{-/-}$tMCAO-5d group. This finding suggests that AR may be associated with inflammation during the acute phase of ischemic stroke, and the absence of AR may reduce inflammation levels.

Autophagy is a cellular defense mechanism that involves the engulfment of waste products and the degradation of broken organelles and proteins within the cell. This process occurs in response to nutrient deprivation and helps to maintain cellular homeostasis [23]. Ischemic stroke injury can cause oxidative stress and mitochondrial dysfunction, as shown in previous research [7]. Autophagy markers such as Beclin-1, LC3B, and P62 are commonly used [11]. While Beclin-1 and LC3B are believed to promote autophagy, not all

cells that upregulate Beclin-1 are necessarily destined to die [24]. Autophagy involves the enzymatic decomposition of a small segment of polypeptide by cytoplasmic LC3 (LC3I), which transforms it into an autophagosome membrane type (LC3B). While moderate activation of autophagy can prevent ischemic neuronal damage to a certain extent, excessive autophagy may lead to cell death [25]. P62 is an autophagy receptor that binds to protein sites and facilitates the degradation of ubiquitinated proteins [26]. In this study, the expression of autophagy initiation and maturation markers was detected to investigate whether AR loss affects the expression of autophagy markers in ischemic stroke. Beclin-1 expression was increased in the WT tMCAO-1d group compared with the WT sham group. Autophagy activation increased in WT mice subjected to cerebral ischemia. Notably, Beclin-1 expression was decreased in the $AR^{-/-}$ tMCAO-1d and $AR^{-/-}$ tMCAO-3d groups compared with that in the $AR^{-/-}$ sham group. Beclin-1 is a molecule involved in the initiation of autophagy. $AR^{-/-}$ mice experienced reduced autophagy initiation after cerebral ischemia. We speculate that Beclin-1, a marker of autophagy-related vesicular formation, has a potential association with AR. This results in a reduction in the overactivation of autophagy after tMCAO, and the lysosome reduces the metabolism of normal organelles, maintains an appropriate degree of autophagy, prevents excessive autophagy, and helps to maintain a stable intracellular environment. On Days 1 and 3 after tMCAO, the $AR^{-/-}$ tMCAO group exhibited increased expression of inflammatory factors and increased autophagy but decreased Beclin-1 expression. However, on Day 5 after tMCAO, Beclin-1, LC3B and P62 expression in the $AR^{-/-}$ tMCAO group was not significantly different from that in the $AR^{-/-}$ sham group, indicating that AR loss gradually hindered the activation of autophagy.

Oxidative stress is a pathological condition resulting from the overproduction of reactive oxygen species (ROS). This imbalance between ROS production and elimination can lead to the impairment of normal cellular function [27]. High oxygen consumption in the brain increases the vulnerability of the central nervous system to oxidative stress. Studies have shown that oxidative damage to the brain increases during the progression of neurodegenerative diseases, cerebrovascular diseases, and psychiatric disorders [28]. In cells, antioxidant enzymes such as SOD and glutathione peroxidase (GSH-px) work in combination with other proteins to eliminate harmful molecules such as O^{2-}, H_2O_2, and other peroxides, thereby reducing oxidative damage within the cells [29]. NOX4 is an isoform belonging to the NOX family of enzymes responsible for producing ROS. Elevated NOX4 can cause oxidative stress-induced lipid peroxidation and mitochondrial metabolic disorders [30]. The levels of the antioxidants SOD and GSH-px were significantly reduced in ischemic tissue in the $AR^{-/-}$ tMCAO group, while NOX4 levels were significantly increased on Days 3 and 5. These findings suggest that oxidative stress was activated and antioxidant levels were reduced in the acute phase after tMCAO. However, NOX4 expression did not increase 1 day after stroke, possibly because AR deficiency slowed NOX4 production.

Recent studies have demonstrated that inadequate blood supply to the brain can result in synaptic damage and mitochondrial dysfunction [19,31]. PSD95, a protein located in the postsynaptic density, plays a crucial role in synaptic maturation and is believed to be closely linked to schizophrenia and autism [32,33]. Moreover, PSD95 is a key component involved in glutamatergic transmission during nerve growth and development [34]. Recent studies have confirmed that the selective blocking of hypoxia-induced binding of nNOS to PSD95 using specific drugs has neuroprotective effects in vitro [35]. This highlights the importance of PSD95 in learning and memory in the central nervous system, as it is a critical protein that reflects synaptic plasticity. Additionally, TOM20, a mitochondrial import receptor subunit, plays a crucial role in mitochondrial biogenesis. When TOM20 is defective, it may lead to mitochondrial dysfunction and ultimately neurodegeneration [36,37]. TOM20 can be used as a marker to study mitochondria [38]. PSD95, which is responsible for synaptic plasticity, and the mitochondrial translocase TOM20 were reduced after ischemic stroke. This reduction can be attributed to damage to the postsynaptic membrane and mitochondria in the affected brain tissue. Furthermore, mitochondrial translocase gradually recovered on Days 3 and 5 after ischemic stroke, but the postsynaptic membrane was relieved on Day 5, indicating that in the absence of AR, mitochondria recovered before the postsynaptic membrane, and synaptic damage did not worsen with time. Therefore, we hypothesize that the repair response in ischemic stroke starts from the mitochondria, allowing the cell to receive sufficient energy to repair the rest of the cytoskeleton and organelles.

This study has several limitations. The $AR^{-/-}$ mice in this study were assayed only 1, 3, and 5 days after tMCAO; thus, the long-term impact of AR gene deletion in the tMCAO model was not detected and a longer time period should be used in future experiments. In addition, stroke can be divided into ischemic stroke and hemorrhagic stroke, and the tMCAO model is used only as a model of ischemic stroke. In the future, WT mice and $AR^{-/-}$ mice can be used to establish hemorrhagic stroke models to explore the influence of the AR gene on hemorrhagic stroke.

In summary, $AR^{-/-}$ mice suffered neurological impairment after cerebral ischemia–reperfusion injury, with the most severe brain damage occurring on the first day after tMCAO. On Days 1 and 3 after tMCAO, the levels of inflammation and oxidative stress markers in the ischemic brain tissue of $AR^{-/-}$ mice were increased, synaptic damage was severe, Beclin-1 and P62 expression was reduced, and LC3B expression was increased. On Day 5 after tMCAO, the expression of Beclin-1, P62 and LC3B in the ischemic brain tissue of the $AR^{-/-}$ mice improved. This study used $AR^{-/-}$ mice to investigate the changes in autophagy factors in the brain tissue of mice with ischemic stroke caused by AR deficiency and to provide laboratory evidence for the use of AR inhibitors in patients with ischemic stroke.

Funding

This work was supported by the National Natural Science Foundation of China (No. 82160946 and No. 81904104), the Natural Science Foundation of Guangdong Province of China (No. 2023A1515012174), the Guangzhou Basic and Applied Basic Research Foundation / Science and Technology Program of Guangzhou City of China (No. 2023A03J0744), the Guangdong Provincial Key Laboratory of Research on Emergency in TCM (No. YN2023JZ17), the Science and Technology Planning Project of Guangdong Province (No. 2023B1212060062), the State Key Laboratory of Traditional Chinese Medicine Syndrome (No. QZ2023ZZ31), and Research Fund for Zhaoyang Talents of Guangdong Provincial Hospital of Chinese Medicine (No. ZY2022KY06).

Ethics approval and consent to participate

This study was reviewed and approved by the Animal Ethics Committee at Guangdong Hospital of Traditional Chinese Medicine, with the approval number: 2019049.

Data availability statement

The data will be made available upon request.

CRediT authorship contribution statement

Jie Li: Writing – original draft, Resources, Funding acquisition, Data curation, Conceptualization. **Zhenqiu Ning:** Writing – review & editing, Writing – original draft, Investigation, Formal analysis, Data curation. **Xiaoqin Zhong:** Writing – original draft, Formal analysis, Data curation. **Dafeng Hu:** Methodology, Data curation. **Yu Wang:** Data curation. **Xiao Cheng:** Writing – review & editing, Supervision, Investigation, Conceptualization. **Minzhen Deng:** Writing – review & editing, Writing – original draft, Validation, Supervision, Methodology, Investigation, Funding acquisition, Formal analysis, Data curation, Conceptualization.

Declaration of competing interest

The authors declare that they have no known competing financial interests or personal relationships that could have appeared to influence the work reported in this paper.

Appendix A. Supplementary data

Supplementary data to this article can be found online at https://doi.org/10.1016/j.heliyon.2024.e38068.

References

[1] J.H. Sun, L. Tan, J.T. Yu, Post-stroke cognitive impairment: epidemiology, mechanisms and management, Ann. Transl. Med. 2 (8) (2014) 80. http://10.3978/j.issn.2305-5839.2014.08.05.
[2] X. Zhang, M. Wei, J. Fan, W. Yan, X. Zha, H. Song, et al., Ischemia-induced upregulation of autophagy preludes dysfunctional lysosomal storage and associated synaptic impairments in neurons, Autophagy 17 (6) (2021) 1519–1542. http://10.1080/15548627.2020.1840796.
[3] Z. Zhou, J. Lu, W.W. Liu, A. Manaenko, X. Hou, Q. Mei, et al., Advances in stroke pharmacology, Pharmacol. Ther. 191 (2018) 23–42. http://10.1016/j.pharmthera.2018.05.012.
[4] A. Chamorro, U. Dirnagl, X. Urra, A.M. Planas, Neuroprotection in acute stroke: targeting excitotoxicity, oxidative and nitrosative stress, and inflammation, Lancet Neurol. 15 (8) (2016) 869–881. http://10.1016/S1474-4422(16)00114-9.
[5] G.R. De Meyer, M.O. Grootaert, C.F. Michiels, A. Kurdi, D.M. Schrijvers, W. Martinet, Autophagy in vascular disease, Circ. Res. 116 (3) (2015) 468–479. http://10.1161/CIRCRESAHA.116.303804.
[6] Q.Q. Guo, S.S. Wang, S.S. Zhang, H.D. Xu, X.M. Li, Y. Guan, et al., ATM-CHK2-Beclin 1 axis promotes autophagy to maintain ROS homeostasis under oxidative stress, EMBO J. 39 (10) (2020) e103111. http://10.15252/embj.2019103111.
[7] Y. Zhang, Y. Cao, C. Liu, Autophagy and ischemic stroke, Adv. Exp. Med. Biol. 1207 (2020) 111–134. http://10.1007/978-981-15-4272-5_7.
[8] P.D. Stanzione R, M. Cotugno, M. Forte, S. Rubattu, Role of autophagy in ischemic stroke: insights from animal models and preliminary evidence in the human disease, Front. Cell Dev. Biol. 12 (2024) 1360014. http://10.3389/fcell.2024.1360014.
[9] H.G. Peng L, Q. Yao, J. Wu, Z. He, B.Y. Law, G. Hu, X. Zhou, J. Du, A. Wu, L. Yu, Microglia autophagy in ischemic stroke: a double-edged sword, Front. Immunol. 13 (2022) 1013311. http://10.3389/fimmu.2022.1013311.
[10] W.S. Ajoolabady A, G. Kroemer, J.M. Penninger, V.N. Uversky, D. Pratico, N. Henninger, R.J. Reiter, A. Bruno, K. Joshipura, H. Aslkhodapasandhokmabad, D. J. Klionsky, J. Ren, Targeting autophagy in ischemic stroke: from molecular mechanisms to clinical therapeutics, Pharmacol. Ther. 225 (2021) 107848. http://10.1016/j.pharmthera.2021.107848.
[11] M. Deng, X. Zhong, Z. Gao, W. Jiang, L. Peng, Y. Cao, et al., Dynamic changes in Beclin-1, LC3B and p62 at various time points in mice with temporary middle cerebral artery occlusion and reperfusion (tMCAO), Brain Res. Bull. 173 (2021) 124–131. http://10.1016/j.brainresbull.2021.05.002.
[12] S.S. Chung, S.K. Chung, Aldose reductase in diabetic microvascular complications, Curr. Drug Targets 6 (2005) 475–486.
[13] S. Thakur, S.K. Gupta, V. Ali, P. Singh, M. Verma, Aldose Reductase: a cause and a potential target for the treatment of diabetic complications, Arch Pharm. Res. (Seoul) 44 (7) (2021) 655–667. http://10.1007/s12272-021-01343-5.
[14] M. Deng, J. Sun, L. Peng, Y. Huang, W. Jiang, S. Wu, et al., Scutellarin acts on the AR-NOX axis to remediate oxidative stress injury in a mouse model of cerebral ischemia/reperfusion injury, Phytomedicine 103 (2022) 154214. http://10.1016/j.phymed.2022.154214.
[15] A.C. Lo, A.K. Cheung, V.K. Hung, C.M. Yeung, Q.Y. He, J.F. Chiu, et al., Deletion of aldose reductase leads to protection against cerebral ischemic injury, J Cereb Blood Flow Metab 27 (8) (2007) 1496–1509. http://10.1038/sj.jcbfm.9600452.
[16] A. Lasek-Bal, H. Jedrzejowska-Szypulka, S. Student, A. Warsz-Wianecka, K. Zareba, P. Puz, et al., The importance of selected markers of inflammation and blood-brain barrier damage for short-term ischemic stroke prognosis, J. Physiol. Pharmacol. 70 (2) (2019). http://10.26402/jpp.2019.2.04.
[17] A.R. Tso, J.G. Merino, S. Warach, Interleukin-6 174G/C polymorphism and ischemic stroke: a systematic review, Stroke 38 (11) (2007) 3070–3075. http://10.1161/STROKEAHA.107.492231.
[18] F. Purroy, J. Farre-Rodriguez, G. Mauri-Capdevila, M. Vicente-Pascual, J. Farre, Basal IL-6 and S100b levels are associated with infarct volume, Acta Neurol. Scand. 144 (5) (2021) 517–523. http://10.1111/ane.13487.
[19] K. Yamagata, Astrocyte-induced synapse formation and ischemic stroke, J. Neurosci. Res. 99 (5) (2021) 1401–1413. http://10.1002/jnr.24807.
[20] A. Patabendige, A. Singh, S. Jenkins, J. Sen, R. Chen, Astrocyte activation in neurovascular damage and repair following ischaemic stroke, Int. J. Mol. Sci. 22 (8) (2021). http://10.3390/ijms22084280.
[21] Y. Zhao, B. Deng, Y. Li, L. Zhou, L. Yang, X. Gou, et al., Electroacupuncture pretreatment attenuates cerebral ischemic injury via notch pathway-mediated up-regulation of hypoxia inducible factor-1alpha in rats, Cell. Mol. Neurobiol. 35 (8) (2015) 1093–1103. http://10.1007/s10571-015-0203-9.

[22] M.P. Mattson, C. Culmsee, Z.F. Yu, Apoptotic and antiapoptotic mechanisms in stroke, Cell Tissue Res. 301 (1) (2000) 173–187. http://10.1007/s004419900154.
[23] H. Wasan, D. Singh, B. Joshi, U. Sharma, A.K. Dinda, K.H. Reeta, Post stroke safinamide treatment attenuates neurological damage by modulating autophagy and apoptosis in experimental model of stroke in rats, Mol. Neurobiol. 58 (12) (2021) 6121–6135. http://10.1007/s12035-021-02523-6.
[24] A. Rami, A. Langhagen, S. Steiger, Focal cerebral ischemia induces upregulation of Beclin 1 and autophagy-like cell death, Neurobiol. Dis. 29 (1) (2008) 132–141. http://10.1016/j.nbd.2007.08.005.
[25] Y. Mo, Y.Y. Sun, K.Y. Liu, Autophagy and inflammation in ischemic stroke, Neural Regen Res 15 (8) (2020) 1388–1396. http://10.4103/1673-5374.274331.
[26] Y. Katsuragi, Y. Ichimura, M. Komatsu, p62/SQSTM1 functions as a signaling hub and an autophagy adaptor, FEBS J. 282 (24) (2015) 4672–4678. http://10.1111/febs.13540.
[27] C. Gorrini, I.S. Harris, T.W. Mak, Modulation of oxidative stress as an anticancer strategy, Nat. Rev. Drug Discov. 12 (12) (2013) 931–947. http://10.1038/nrd4002.
[28] S. Salim, Oxidative stress and the central nervous system, J Pharmacol Exp Ther 360 (1) (2017) 201–205. http://10.1124/jpet.116.237503.
[29] G. Filomeni, D. De Zio, F. Cecconi, Oxidative stress and autophagy: the clash between damage and metabolic needs, Cell Death Differ. 22 (3) (2015) 377–388. http://10.1038/cdd.2014.150.
[30] M.W. Park, H.W. Cha, J. Kim, J.H. Kim, H. Yang, S. Yoon, et al., NOX4 promotes ferroptosis of astrocytes by oxidative stress-induced lipid peroxidation via the impairment of mitochondrial metabolism in Alzheimer's diseases, Redox Biol. 41 (2021) 101947. http://10.1016/j.redox.2021.101947.
[31] H. An, B. Zhou, X. Ji, Mitochondrial quality control in acute ischemic stroke, J Cereb Blood Flow Metab 41 (12) (2021) 3157–3170. http://10.1177/0271678X211046992.
[32] A.A. Coley, W.-J. Gao, PSD95: a synaptic protein implicated in schizophrenia or autism? Prog. Neuro Psychopharmacol. Biol. Psychiatr. 82 (2018) 187–194. http://10.1016/j.pnpbp.2017.11.016.
[33] T.M. Hu, C.L. Wu, S.H. Hsu, H.Y. Tsai, F.Y. Cheng, M.C. Cheng, Ultrarare loss-of-function mutations in the genes encoding the ionotropic glutamate receptors of kainate subtypes associated with schizophrenia disrupt the interaction with PSD95, J Pers Med 12 (5) (2022). http://10.3390/jpm12050783.
[34] L. Liu, L. Dai, D. Xu, Y. Wang, L. Bai, X. Chen, et al., Astrocyte secretes IL-6 to modulate PSD-95 palmitoylation in basolateral amygdala and depression-like behaviors induced by peripheral nerve injury, Brain Behav. Immun. 104 (2022) 139–154. http://10.1016/j.bbi.2022.05.014.
[35] L. Zhou, F. Li, H.B. Xu, C.X. Luo, H.Y. Wu, M.M. Zhu, et al., Treatment of cerebral ischemia by disrupting ischemia-induced interaction of nNOS with PSD-95, Nat Med 16 (12) (2010) 1439–1443. http://10.1038/nm.2245.
[36] M.G. Nasoni, S. Carloni, B. Canonico, S. Burattini, E. Cesarini, S. Papa, et al., Melatonin reshapes the mitochondrial network and promotes intercellular mitochondrial transfer via tunneling nanotubes after ischemic-like injury in hippocampal HT22 cells, J. Pineal Res. 71 (1) (2021) e12747. http://10.1111/jpi.12747.
[37] N.T. Nhu, S.Y. Xiao, Y. Liu, V.B. Kumar, Z.Y. Cui, S.D. Lee, Neuroprotective effects of a small mitochondrially-targeted tetrapeptide elamipretide in neurodegeneration, Front. Integr. Neurosci. 15 (2021) 747901. http://10.3389/fnint.2021.747901.
[38] Y.N. Dou, X. Wu, X. Fei, Z. Fei, The neuroprotective effect of increased PINK1 expression following glutamate excitotoxicity in neuronal cells, Neuroscience 480 (2022) 97–107. http://10.1016/j.neuroscience.2021.11.020.